Experiment 3: Photoluminescence Spectroscopy of Semiconductors

Anand Hari Natarajan and Parth Himanshu Pathak

I. Introduction

According to the Band Theory of solids, all solids have in them a large number of electrons whose orbitals overlap to become very closely spaced in energy. The various discrete energy levels that are usually present in different orbitals now produce a continuous spectra or an energy "band". The reason why certain solids are electrical conductors whereas others are not, can be explained using this theory. It explains that in certain materials, there is a continuous band of energy values beyond a certain maximum energy that cannot be assumed by the electrons due to a "band gap" energy and are therefore "forbidden". The band gap causes electrons to naturally be bound to the lower energy spectra. The higher forbidden energy band is called the "conduction band" and the lower accessible energy band is called the "valence band". What this means physically is that in solids, the electrons are bound to the atoms and have certain values of energy in the valence band. If provided with a external perturbative excitation, the electrons in the outermost energy level in the valence band gain enough energy to "jump" across the band gap to access the conduction band, becoming free to move through the lattice to conduct electric currents. In some materials though, the band gap is too wide for any excitation to produce electron jumps. These materials are called "Insulators" whereas the materials where the energy gap is small enough to facilitate jumps across it are called "Semiconductors".

The goal of this experiment is to use laser light to investigate the band gap energies in semiconductor materials by performing photoluminescence (PL) spectroscopy. Specifically, PL spectroscopy is used:
a. To find the band gap energies of the given samples of GaAs, InP, and $In_{1-x}Ga_xP$,
b. To calculate the alloy concentration in $In_{1-x}Ga_xP$.
c. To measure their average diameters of a sample of CdTe nanoparticles,

Using laser light is an example of photo-excitation where, if the incident photons have energies larger than the band gap, the electrons in the valence band would jump to the conduction band and still have some energy to spare. The electrons then slowly lose the excess energy and fall to the lowest energy level in the conduction band and then finally fall back to the highest energy level in the valence band. In the process of taking its place in the valence band, the electron loses energy equal to the band gap, which is released in the form of photons. The energy of these photons, if measured can tell one the band gap energy for the particular material. This process where the material is excited using photons causing it to emit photons itself is called "photoluminescence".

II. <u>Materials and Methods</u>

A. <u>Materials</u>

A. I. The experimental setup

A schematic diagram of the experimental setup is shown in Figure 1. The solid aluminum optical breadboard with 1/4-20 tapped holes was used as the baseplate for the experimental setup. A 5mW 530 nm green laser diode was used as the light source. A focusing lens (convex lens of 200 mm focal length) was used for focusing the laser beam onto a mirror. The mirror was used to direct the laser light onto the semiconductor sample. Semiconductor samples of GaAs, InP, $In_{1-x}Ga_xP$, and CdTe nanoparticles were used for the experiment. The first three samples were mounted on a metal plate one above the other. The CdTe nanoparticles sample consisted of CdTe quantum dots on a microscope slide with a cover slip on top of it. The whole sample was further mounted on a metal plate. A collection lens (convex lens of 25 mm focal length) was used for focusing the photons emitted by the semiconductor sample into the optical aperture through the 590 nm long-pass optical filter. The filter absorbs photons of wavelength below 590 nm and allows photons of wavelength above 590 nm to pass through it. The filter also serves the purpose of filtering out any residual green light from the laser. The optical aperture was used to send the photons emitted by the sample into a 600 micron core optical fiber cable, which then sends the light into the spectrometer. The spectrometer used was the model USB2000-FLG by Ocean Optics. The spectrometer was connected to the computer using a USB cable. The OceanView software (from www.oceaninsight.com) was used for spectral analysis. Optical posts and post holders were used to fasten all the different components onto the breadboard. A picture of the actual experimental setup is included in the Appendix section.
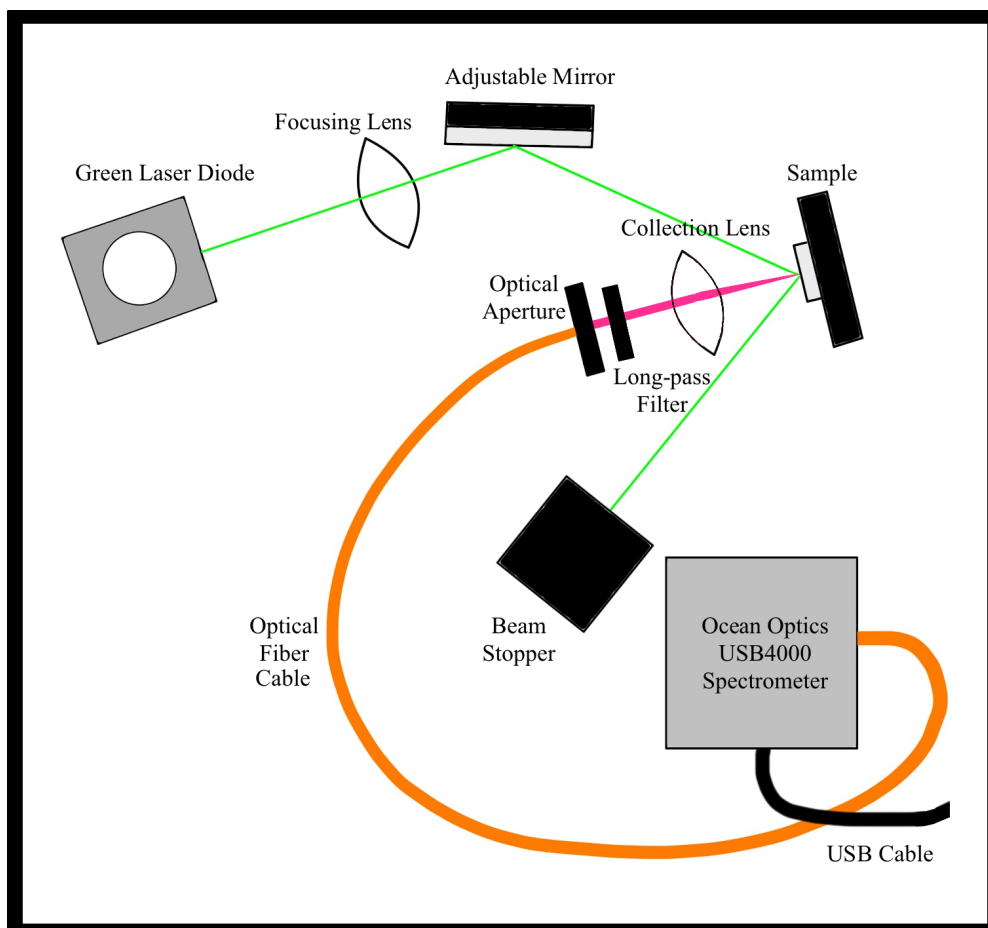

Figure 1: Schematic Diagram of the experimental setup

B. Methods

B. I. PL spectroscopy of ambient light from fluorescent tube

In this experiment, PL spectroscopy of ambient light was performed. One end of the optical fibre cable was connected to the spectrometer, while the other end was directed towards one of the room walls to collect the stray light reflected off it. The OceanView software was started and the 'Integration Time' option was adjusted to 4375 μs such that the highest peak was just below 4000 counts. The 'Scans to Average' option was set to 15 and the 'Boxcar width' option was set to 5 to smoothen out the random errors.

B. II. Assembling the optical setup

All the optical components were placed firmly onto the breadboard as in Figure 1. Usually a Neutral Density (ND) optical filter (a filter that reduces laser intensity) is added between the laser source and the adjustable mirror. For this experiment, an ND optical filter that reduced intensity by 10x was available but was not added since the intensity of the resultant spectral lines were too low. The heights and orientations of all the components were adjusted by loosening and fastening the screws on the optical post holders.

The placements of the optical lenses in the setup are calculated using the 'lens equation'. The lens equation relates the position of the object from the center of the lens to the position of the image from the center of the lens using the focal length of the convex lens.

$$\frac{1}{u} + \frac{1}{v} = \frac{1}{f}$$

Here, u is the object distance measured from the centre of the lens, v is the image distance measured from the centre of the lens, and f is the focal length of the convex lens.

The magnification for the lens is given by $M = \dfrac{v}{u}$.

In the special case of focusing a collimated laser beam using a convex lens, the object distance from the center of the lens is considered to be infinite since all rays of light coming from the source are assumed to be parallel to each other.

Plugging in $u \rightarrow \infty$ into the lens equation gives us $\dfrac{1}{v} = \dfrac{1}{f}$ or $v = f$.

This means that our image is formed at the focus of the lens. Furthermore, we can also see that the magnification $M \rightarrow 0$. This means that the image is focused to a point.

In the experiment, two convex lenses were used: the 'focusing lens' of focal length 200 mm to focus light onto a mirror which reflects it onto the semiconductor samples, and the 'collection lens' of focal length 25 mm, which was used to focus the photoluminescence from the samples into the optical aperture. For the focusing lens, the laser light gets focused to a point exactly 200 mm from the centre of the lens and so the mirror is placed at approximately 200 mm from the lens. In the case of the collection lens, the sample is placed 25 mm from the center of the collection lens so that the photoluminescence is gathered into a collimated beam that can be approximated as parallel rays of

light traveling to infinity. This collimated beam travels through the optical aperture and into the optical fiber cable.

B. III. Calibrating the optical setup

After the setup was assembled, the collection lens's position was calibrated with respect to the sample's position. This was done to make sure that the sample was placed at the focal length of the collection lens. Calibration was done by disconnecting the optical fibre cable from the spectrometer and passing white light from a torch into it. The position of the lens and aperture were then adjusted with respect to the sample such that the white light was focused to a dot on it. The mirror's angle was then adjusted such that the laser coincided with the dot. A black cloth was used to cover the whole setup and shield it from the ambient light. Further fine adjustments were made to the heights and angles by adjusting the screws under the cloth to maximize the PL spectral peak.

B. IV. Calculating the PL spectral peak of GaAs

The height of the sample was adjusted such that the laser light fell on the GaAs sample. The OceanView software was used to analyze the PL spectrum of GaAs. The 'Integration Time' option was set to 20 ms. The 'Scans to Average' option was set to 15 and the 'Boxcar width' option was set to 5 to smoothen out the random errors. The wavelength at which the spectral peak occurred and full-width at half-maximum (FWHM) line-width were measured.
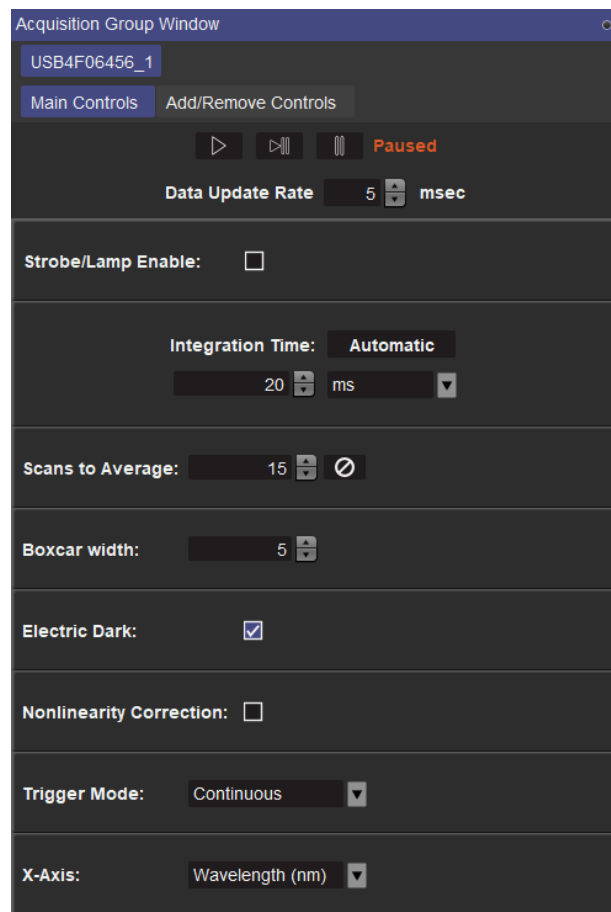

Figure 2: The settings for PL spectroscopy of GaAs

B. V. Calculating the PL spectral peak of InP

Next, the height of the sample was adjusted such that the laser light fell on the InP sample. The OceanView software was used to analyze the PL spectrum of InP. The 'Integration Time' option was set to 240 ms. The 'Scans to Average' option was set to 10 and the 'Boxcar width' option was set to 5 to smoothen out the random errors. The wavelength at which the spectral peak occurred and full-width at half-maximum (FWHM) line-width were measured.
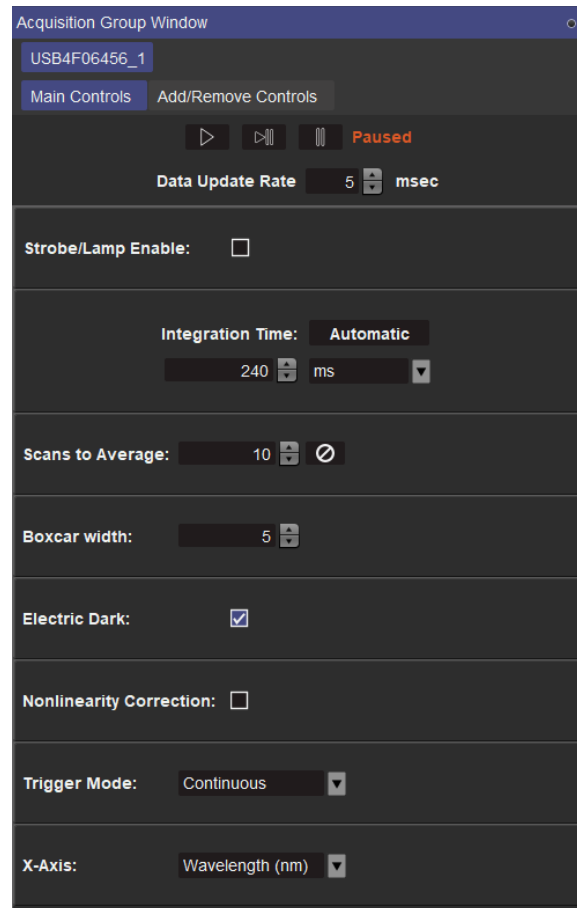

Figure 3: The settings for PL spectroscopy of InP

B. VI. Calculating the PL spectral peak of $In_{1-x}Ga_xP$

Finally, the height of the sample was adjusted such that the laser light fell on the $In_{1-x}Ga_xP$ sample. The OceanView software was used to analyze the PL spectrum of $In_{1-x}Ga_xP$. The 'Integration Time' option was set to 2000 μs. The 'Scans to Average' option was set to 15 and the 'Boxcar width' option was set to 5 to smoothen out the random errors. The wavelength at which the spectral peak occurred and full-width at half-maximum (FWHM) line-width were measured.
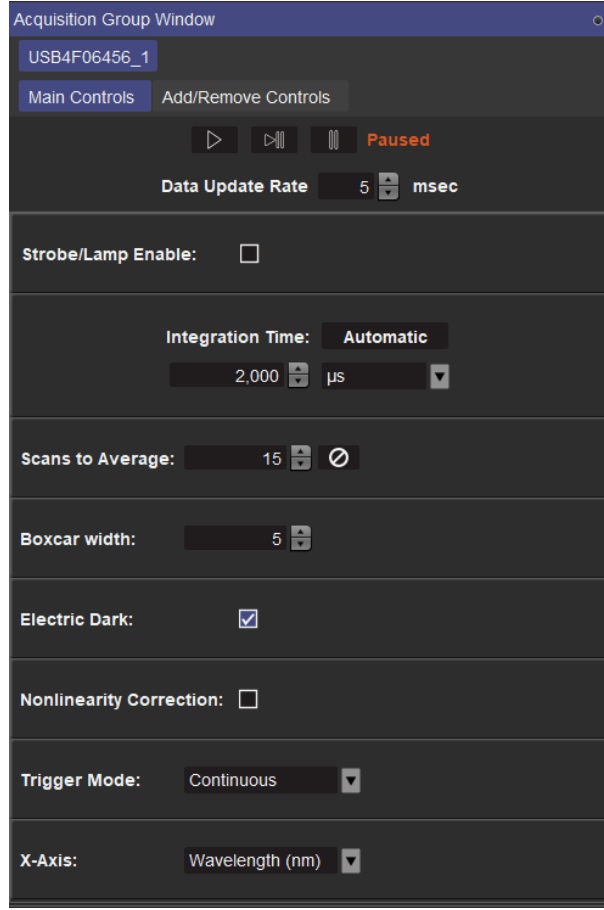
Figure 4: The settings for PL spectroscopy of $In_{1-x}Ga_xP$

B. VII. Determining gallium concentration in $In_{1-x}Ga_xP$

To determine the concentration of gallium in the semiconductor alloy $In_{1-x}Ga_xP$, its PL spectral peak was compared to that of InP. The band gap energy of a material can be changed by alloying and in this case, some In atoms were replaced by Ga atoms.
The band gap energy of $In_{1-x}Ga_xP$ can be modeled as a polynomial function of the gallium concentration x as follows:

$$E'(x) = E_0 + 512x + 603x^2$$

Here, E' is the band gap energy of $In_{1-x}Ga_xP$ in units of meV and E_0 is the band gap energy of InP in units of meV.

B. VIII. Determining the average diameter of CdTe nanoparticles

Usually for this part of the experiment, the previous metal plate containing the three semiconductor samples is replaced with the metal plate containing the CdTe sample and its height is adjusted so that the laser falls on it. Then the OceanView software is used to analyze the sample's PL spectrum. However, the CdTe sample was missing and so the spectral data was acquired from the Teaching Assistant. Using the data, the wavelength at which the spectral peak occurred and full-width at half-maximum (FWHM) line-width were measured.

The band gap energy of a semiconductor material can shift to a higher energy when the size of the material is in the range of 100 nm. The shifted band gap energy can be mathematically calculated using the Brus equation:

$$E_{NP}(x) = E_0 + \frac{\hbar^2 k^2}{2m} = E_0 + \frac{\hbar^2}{2m} \cdot \frac{\pi^2}{d^2}$$

Here, E_{NP} is the band gap energy of the nanoparticles sample in units of meV. E_0 is the band gap energy of the bulk sample calculated to be 1490 meV. m is the effective mass of a "pseudo-electron" and is given by $m = 0.09m_0$, where m_0 is the mass of an electron. k is the wave-vector and for quantum confinement, it can be written as $k = \frac{\pi}{d}$, where d is the diameter of the nanoparticle.

Thus, one can calculate the diameter of the nanoparticle by inverting the above relation.

III. Results

A. PL spectroscopy of ambient light from fluorescent tube

Using OceanView, the spectrum was found to be as shown in Figure 5.
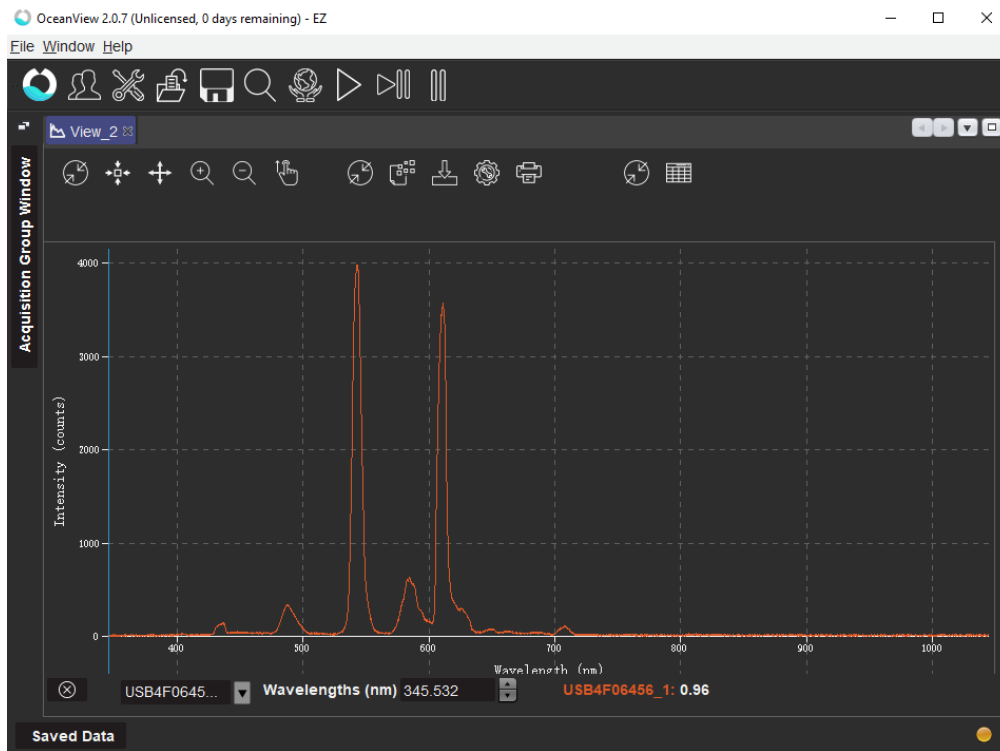

Figure 5: PL spectrum of ambient light from fluorescent tube

As shown in Figure 5, there are six peaks in the PL spectrum. These peaks were found to occur at the following wavelengths in ascending order: 436.404 nm, 487.605 nm, 543.185 nm, 584.643 nm, 611.094 nm, and 708.436 nm. The narrowest line corresponds to peak 5 and its line-width (FWHM) was calculated to be 9.047 nm.

Table 1

	Wavelength (nm)	Intensity (counts/second)	Element
Peak 1	436.404	73138.286	Hg
Peak 2	487.605	166630.857	Tb^{3+}
Peak 3	543.185	909339.429	Tb^{3+}
Peak 4	584.643	264228.571	$Tb^{3+}/Eu^{3+}:Y_2O_3$
Peak 5	611.094	828278.857	$Eu^{3+}:Y_2O_3$
Peak 6	708.436	54253.714	$Eu^{3+}:Y_2O_3$

List of elements corresponding to the six strongest lines in the PL spectrum of ambient light along with their intensities in counts/second

In Table 1, Intensity in counts/second was found by dividing the peaks by the integration time, 4375 μs. The elements for the spectral peaks were found from the NIST database of spectra for mercury [1] and an article on fluorescent light phosphors [2].

B. PL spectroscopy of GaAs

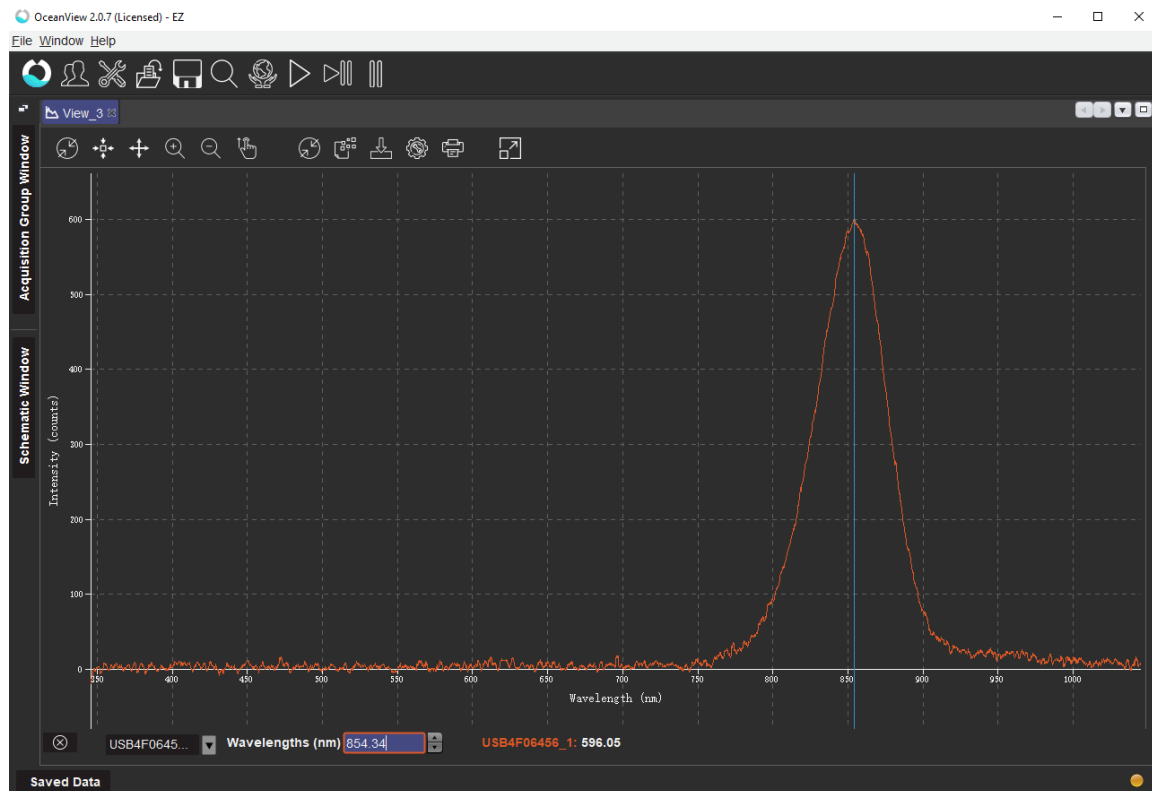Using OceanView, the spectrum was found to be as shown in Figure 6.

Figure 6: PL spectrum of GaAs

The peak was measured to occur at the wavelength **854.34 nm** and the line-width was calculated to be **55.434 nm**.
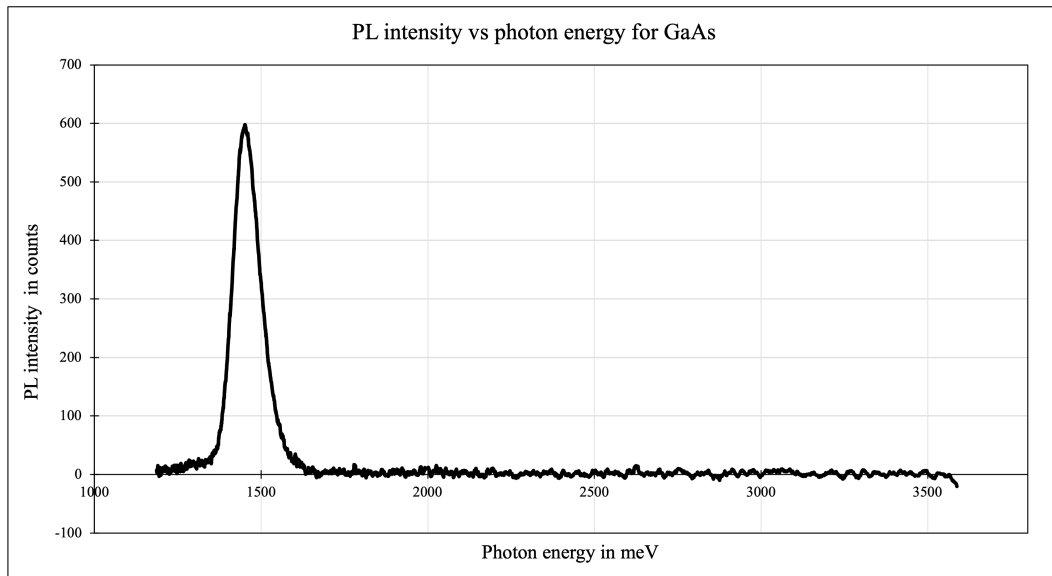

Figure 7: PL intensity vs photon energy for GaAs

The peak in Figure 7 arises at photon energy **1450.843 meV** and the line-width was calculated to be **94.783 meV**. The uncertainty in the peak photon energy is calculated to be **40.248 meV**.

C. PL spectroscopy of InP

Using OceanView, the spectrum was found to be as shown in Figure 8.
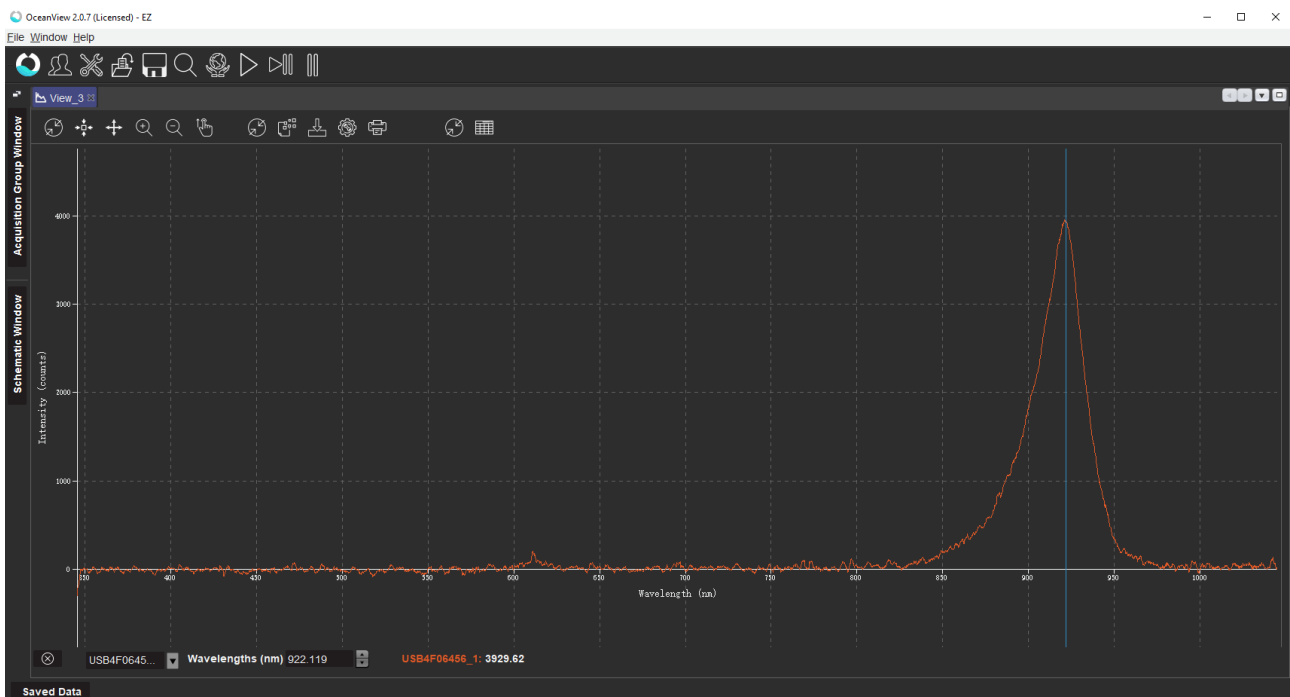

Figure 8: PL spectrum of InP

The peak was measured to occur at the wavelength **922.119 nm** and the line-width was calculated to be **32.648 nm**. The peak also arises at photon energy **1344.200 meV** and the line-width was calculated to be **47.77 meV**. The uncertainty in the peak photon energy is calculated to be equal to **20.284 meV**.

D. PL spectroscopy of In$_{1-x}$Ga$_x$P

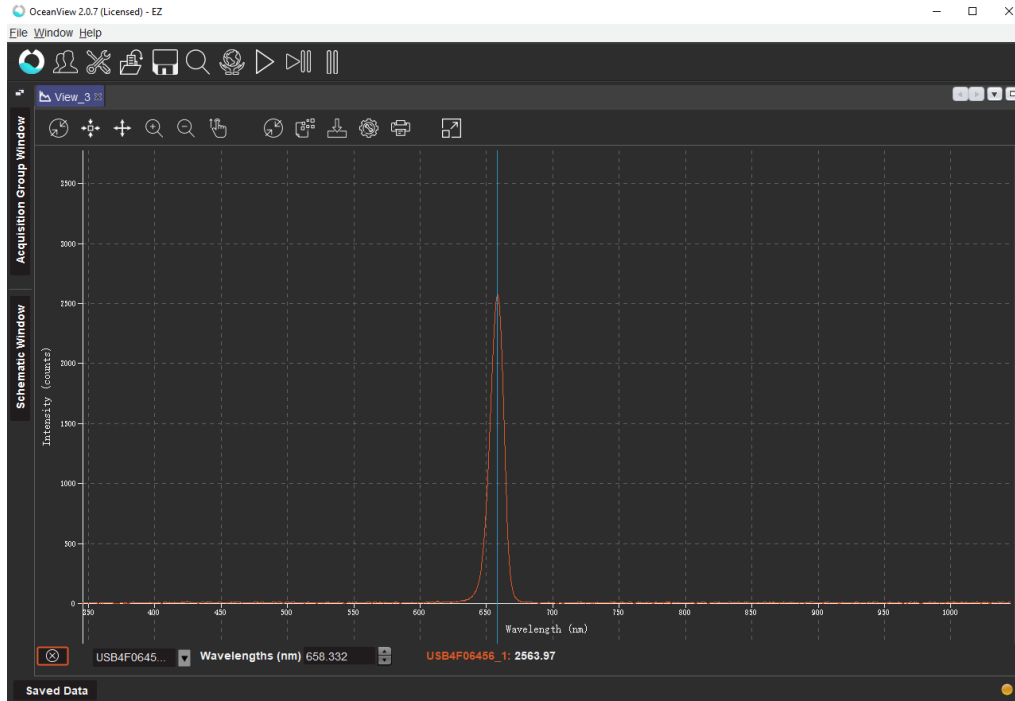Using OceanView, the spectrum was found to be as shown in Figure 9.

Figure 9: PL spectrum of In$_{1-x}$Ga$_x$P

The peak was measured to occur at the wavelength **658.332 nm** and the line-width was calculated to be **11.858 nm**. The peak also arises at photon energy **1882.81 meV** and the line-width was calculated to be **33.958 meV**. The uncertainty in the peak photon energy is calculated to be equal to **14.419 meV**.

E. Calculating gallium concentration in In$_{1-x}$Ga$_x$P

The concentration of gallium can be determined by comparing the photon energy values at which the peaks occur for the PL spectrums of both InP and In$_{1-x}$Ga$_x$P.

Using the formula $E'(x) = E_0 + 512x + 603x^2$ to write x as a function of E_0 and E', the gallium concentration can be calculated.

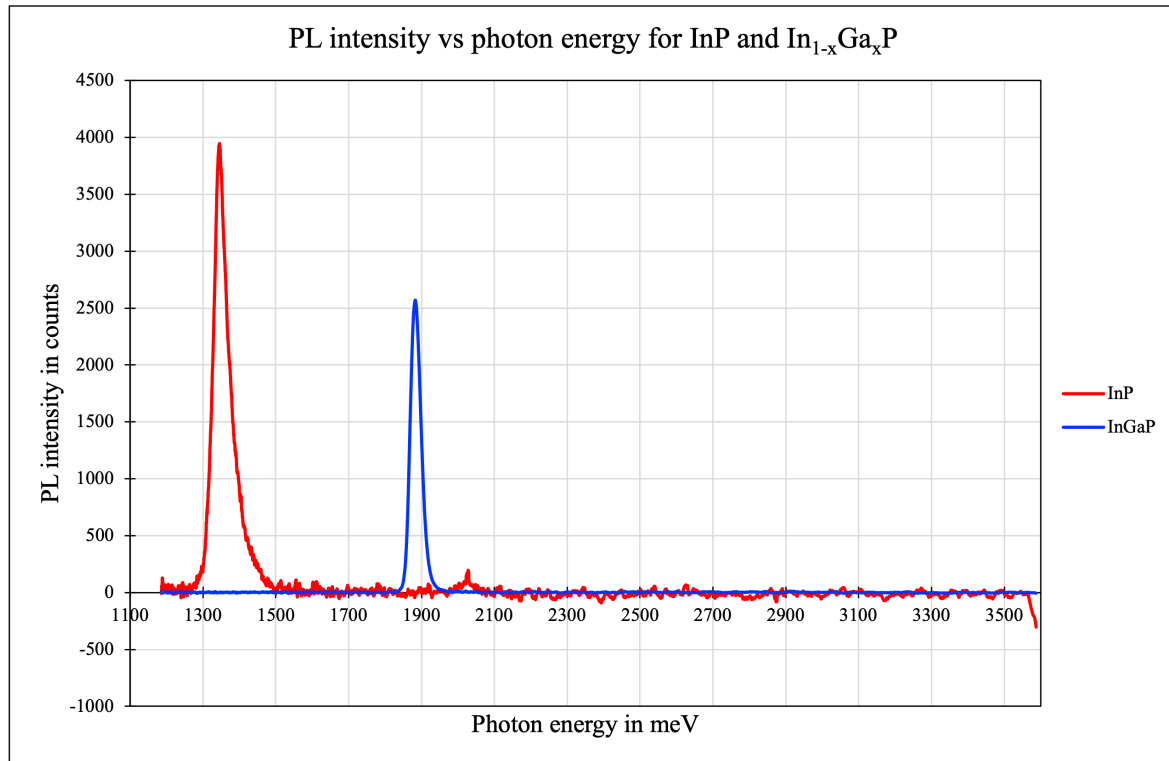$$x(E_0, E') = \frac{-512 \pm \sqrt{(512)^2 + (2412)(E' - E_0)}}{1206}$$

Figure 10: PL intensity vs photon energy for InP and In$_{1-x}$Ga$_x$P

The photon energy value, E_0 at which the spectrum peak occurs for InP is 1344.2 meV. The photon energy value, E' at which the spectrum peak occurs for In$_{1-x}$Ga$_x$P is 1882.81 meV.

Plugging in the values of E_0 and E' into the equation, one gets the following values for gallium concentration:

$$x_{1,2} = 0.6115, -1.4606$$

Since concentration cannot be negative, the second value is ignored. Thus we get $x = 0.6115$. This means that the sample In$_{1-x}$Ga$_x$P is composed of **61.15%** Ga and **38.85%** In.

The uncertainty in x can be calculated using 'propagation of errors' formula (included in the Appendix section). The uncertainty in E_0 is 20.284 meV and in E' it is 14.419 meV.

Using the above data, σ_x is calculated to be **0.02**.
Thus the concentration of gallium is **0.61 ± 0.02**.

The gallium concentration for which the band gap moves to the orange region (590 nm) or $E' = 2100.87$ meV is calculated to be **0.773**.

F. **Calculating the average diameter of CdTe nanoparticles**

The data for the CdTe nanoparticles was provided by the Teaching Assistant and plotted in Excel. The graphs are shown in Figure 11 and 12.
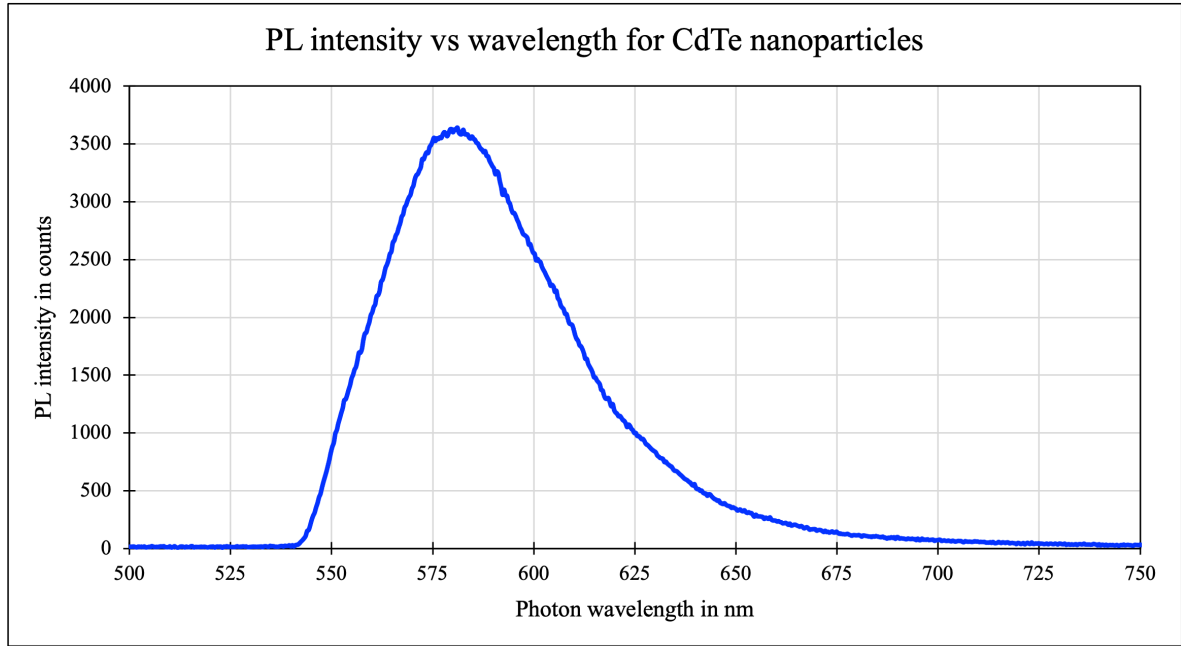
Figure 11: PL intensity vs photon wavelength for CdTe nanoparticles

The photon wavelength for the spectrum peak was calculated as **581.058 nm**. The line-width was found to be **52.747 nm**. The uncertainty in the photon wavelength for peak is **22.398 nm**.
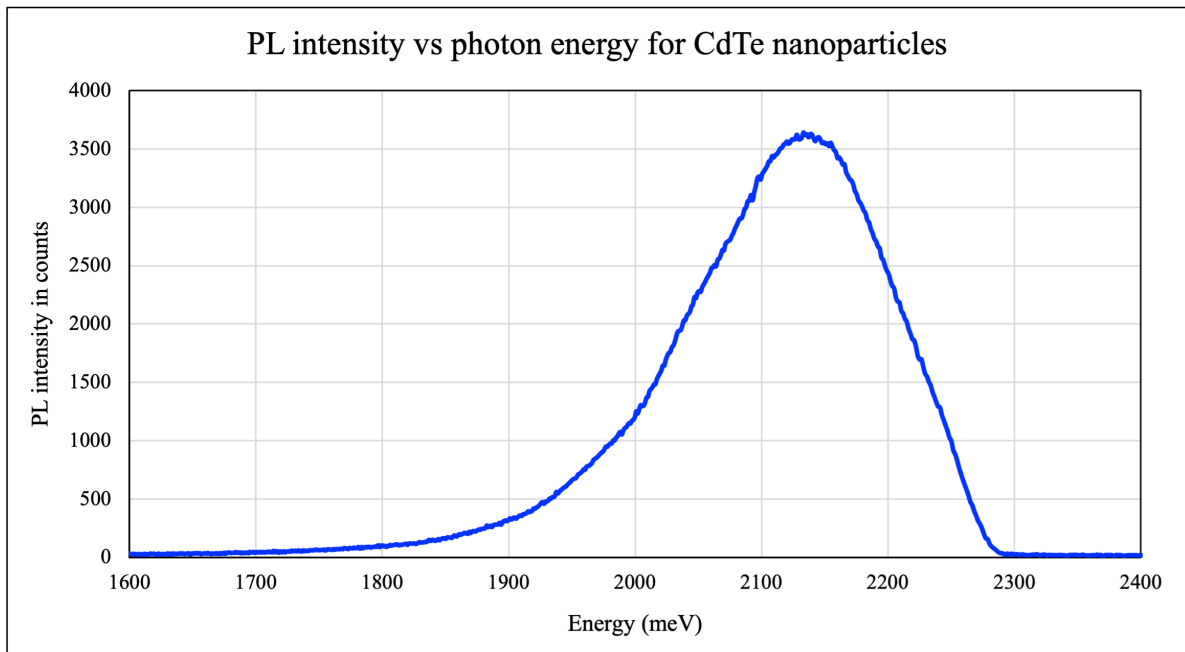

Figure 12: PL intensity vs photon energy for CdTe nanoparticles

The photon energy for the spectrum peak was calculated as **2133.20 meV**. The line-width was found to be **191.97 meV**. The uncertainty in the photon energy for peak is **81.518 meV**.

The average diameter of the CdTe nanoparticles can be calculated using the Brus equation:

$$E_{NP}(x) = E_0 + \frac{\hbar^2 \pi^2}{2m d^2}$$

Rewriting the equation, we get $d^2 = \frac{\hbar^2 \pi^2}{2m(E_{NP} - E_0)}$. Here, E_{NP} and E_0 are 2133.20 meV and 1490 meV respectively and m is $0.09 m_0$.

The diameter is then calculated to be **2.5505 nm**.

The uncertainty in d was found to be **0.1616 nm** using the 'propagation of errors' formula.

Thus the average diameter of the CdTe nanoparticles is **2.5505 ± 0.1616 nm**.

IV. <u>Discussion</u>

A. <u>PL spectroscopy of ambient light from fluorescent tube</u>

The PL spectral analysis of the ambient light emanating from fluorescent tubes revealed that the spectral lines belong to mercury (Hg), terbium (Tb^{3+}), and europium (Eu^{3+}). The strongest spectral line belonged to terbium and europium. These results are as expected since modern fluorescent tubes use terbium-doped $LaPO_4$ and europium-doped Y_2O_3 as phosphors [3]. The spectral lines of mercury were detected since fluorescent tubes typically use a few milligrams of mercury which must be vaporized for the tube to work properly.

B. <u>PL spectroscopy of GaAs</u>

The value of the photon energy corresponding to the spectral peak of GaAs was calculated to be 1.451 eV. This is approximately equal to the well-known energy gap value of 1.424 eV for GaAs at 300 K [4]. Furthermore, the spectral peak has a wavelength of 854.34 nm, which agrees with the fact that GaAs is used for infrared LEDs [5].

C. <u>PL spectroscopy of InP</u>

The value of the photon energy corresponding to the spectral peak of InP was calculated to be 1.344 eV. This is equal to the well-known energy gap value of 1.344 eV for InP at 300 K [4]. Furthermore, the spectral peak has a wavelength of 922.119 nm, which agrees with the fact that InP is used for infrared and microwave communication systems [6].

D. <u>PL spectroscopy of In$_{1-x}$Ga$_x$P</u>

The gallium concentration x was found to be 0.61 ± 0.02. The value of the photon energy corresponding to the spectral peak of $In_{1-x}Ga_xP$ was calculated to be 1.883 eV. This agrees with the fact that doping InP with Ga can increase its band gap energy [7]. In fact, alloying materials with suitable other materials can increase band gap energy [8]. Alloying is a very useful tool to

manipulate band gap energies and change the color of the emitted light. The fact that the spectral peak changed to 658.332 nm, a wavelength in the visible range confirms this.

E. **PL spectroscopy of CdTe nanoparticles**

When the size of particles become approximately less than 100 nm, the band gap energy of the nanoparticles shift to a higher value. This is a result of the quantum mechanical phenomenon called 'quantum confinement'. This effect comes into play when the size of the particle is too small to be comparable to the wavelength of the electron and therefore the movement of the charge carriers are restricted due to the small volume. As a result, electrons or electron-hole pairs called "excitons" are tightly confined in all three dimensions [9]. This confinement has consequences for the electrical, mechanical, and optical properties of the material. It is well known fact that the band gap energy increases of CdTe increases as its size decreases [10].

In this experiment, the diameter of the CdTe nanoparticles was calculated to be 2.55 ± 0.16 nm, which is much smaller than 100 nm and therefore quantum confinement causes a shift in the band gap energy.

V. **Conclusion**

In this experiment, PL spectroscopy was done to analyze the band gap energies of semiconductor samples of GaAs, InP, a sample of InP doped with Ga, and a sample of CdTe nanoparticles. Furthermore, the effect of doping and quantum confinement on band gap energies were studied.

VI. **Appendix**

A. **Optical setup**
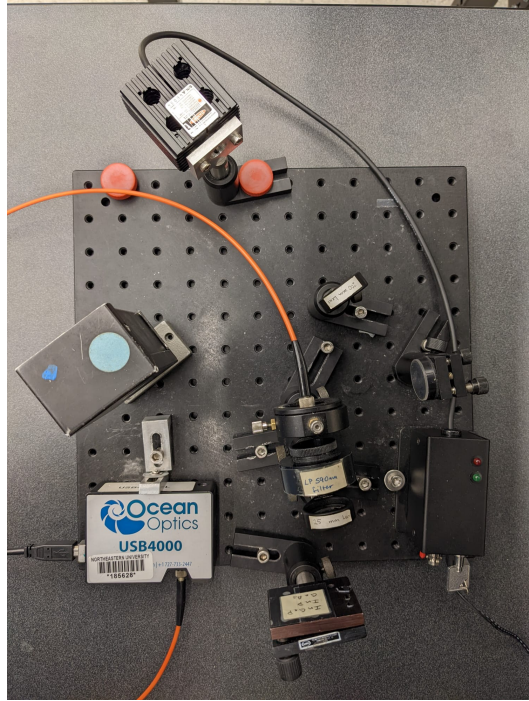

Figure 13: Photo of the actual optical setup

Figure 13 shows the actual optical setup used to conduct the experiment.

B. **Propagation of Errors**

For a random variable x defined as a function of random variables u and v, the 'propagation of errors' formula is as follows:

$$\sigma_x^2 = \sigma_u^2 \left(\frac{\partial x}{\partial u}\right)^2 \Bigg|_{(\bar{u},\bar{v})} + \sigma_v^2 \left(\frac{\partial x}{\partial v}\right)^2 \Bigg|_{(\bar{u},\bar{v})}$$

Here σ_x, σ_u, and σ_v are the uncertainties in x, u, and v respectively. $\bar{u}$ and $\bar{v}$ denote the average values of u and v respectively.

VII. <u>References</u>

1. https://physics.nist.gov/PhysRefData/ASD/lines_form.html

2. https://www.electrochem.org/dl/interface/sum/sum03/IF6-03-Pages48-51.pdf

3. https://www.spectroscopyonline.com/view/fluorescent-lights

4. K. Ng, Complete Guide to Semiconductor Devices, McGraw-Hill, 1995.

5. J. Chatterjee, "Modelling of a GaAs based infrared LED with high efficiency and minimal computation time," *2017 International Conference on Trends in Electronics and Informatics (ICEI)*, 2017, pp. 740-743, doi: 10.1109/ICOEI.2017.8300801.

6. Phelan, R., Byrne, D., O'Carroll, J., Gleeson, M., Nawrocka, M., Lennox, R., Carney, K., Herbert, C., Somers, J., & Kelly, B. (2019). Mid-Infrared InP-Based Discrete Mode Laser Diodes. In G. Huerta-Cuellar, & R. Imani (Eds.), Optical Fiber Applications. IntechOpen. https://doi.org/10.5772/intechopen.86458

7. Schmieder, Nicole. (2022). GROWTH AND ANALYSIS OF GALLIUM PHOSPHIDE ON SILICON FOR VERY HIGH EFFICIENCY SOLAR CELLS.

8. Guisbiers, Gregory & Wautelet, M. & Buchaillot, Lionel. (2009). Phase diagrams and optical properties of phosphide, arsenide, and antimonide binary and ternary III-V nanoalloys. Phys. Rev. B. 79. 10.1103/PhysRevB.79.155426.

9. Chapter 3 - Quantum Nanostructures (QDs): An Overview, Synthesis of Inorganic Nanomaterials, D. Sumanth Kumar, B. Jai Kumar, H. M. Mahesh

10. Pseudopotential Study of CdTe Quantum Dots: Electronic and Optical Properties, Fadila Mezrag, Nadir Bouarissa, https://doi.org/10.1590/1980-5373-MR-2017-1146